Kinetic Modeling Confirms the Biosynthesis of Mucin Core 1 (β-Gal(1−3) α-GalNAc-*O*-Ser/Thr) *O*-glycan Structures Are Modulated by Neighboring Glycosylation Effects†

Thomas A. Gerken*

W. A. Bernbaum Center for Cystic Fibrosis Research, Departments of Pediatrics and Biochemistry, Case Western Reserve University School of Medicine, Cleveland, Ohio 44106

Received December 22, 2003

ABSTRACT: Glycoproteins containing heavily O-glycosylated, mucin-like domains serve important biological functions in which the O-linked glycans play a major role. Although not well understood, *O*-glycan structures are known to vary reproducibly as a function of their position in the peptide sequence. Toward understanding such behavior, an analysis of the in vivo Core 1 (β-Gal(1−3) α-GalNAc-*O*-Ser/Thr) site-specific glycosylation pattern of the porcine salivary gland mucin 81 residue tandem repeat has been undertaken. When a kinetic modeling approach is utilized, the in vivo Core 1 glycosylation pattern could be reproduced by incorporation of the inhibitory effects of neighboring residue glycosylation plus and minus three residues of the site of glycosylation. The obtained positional weighing parameters suggest that the porcine salivary gland Core 1 transferase (UDP-galactose:glycoprotein-α-GalNAc β3-galactosyltransferase) is most sensitive to the presence of glycans C terminal to the site of glycosylation. The analysis further suggests that neighboring peptide core α-GalNAc residues are primarily responsible for the effect. These findings further support the notion that the formation of the Core 1 structure, an important initial step in *O*-glycan biosynthesis, may be regulated to a large extent by neighboring residue glycosylation. As a result, the development of approaches for predicting *O*-glycan core structures in a site-specific manner may now appear a distinct possibility.

Glycoproteins containing heavily O-glycosylated, mucin-like domains play important and diverse biological roles such as protecting cell surfaces, modulating cell−cell interactions, targeting cellular proteins, regulating inflammatory and immune responses, and in tumorogenisis and metastasis (for example, *1*−*7*). In these glycoproteins, O-glycosylated domains typically play critical functional roles, which rely on their extended structures and ability to be decorated by an array of glycan structures (*8*, *9*). In some instances, a unique placement of specific *O*-glycan structures along the peptide sequence may be required for full biological activity (*2*, *10*−*16*). Recently, we have demonstrated that the *O*-glycan structures in the porcine salivary gland mucin (PSM)[1] tandem repeat vary reproducibly as a function of their position in the peptide sequence (*17*). Therefore, the glycosyltransferases that form the initial core *O*-glycan structures as a rule can be expected to display reproducible and specific sensitivities to the peptide sequence. The mechanisms for this modulation of the *O*-glycan structure by peptide sequence is poorly understood, although our previous PSM studies suggest that the presence of neighboring glycans may play a significant role (*17*, *18*). As confirmation, we have recently shown that the site-specific glycosylation of the PSM tandem repeat by purified mammalian UDP-GalNAc:polypeptide α-GalNAc transferases (ppGalNAc transferase) T1 and T2 can be largely reproduced utilizing a kinetic model where the rate of glycosylation is decremented as a function of the neighboring glycosylation state (*19*). We now report that a similar kinetic model can reproduce the in vivo substitution pattern of the peptide α-GalNAc residue by β-Gal [by the action of UDP-galactose: glycoprotein-α-GalNAc β3-galactosyltransferase (Core 1 transferase)] forming the so-called Core 1 basic structure, β-Gal(1−3) α-GalNAc-*O*-Ser/Thr. These findings strongly support the idea that the formation of the Core 1 structure, an important initial step in *O*-glycan biosynthesis, may be highly modulated, if not regulated, by neighboring glycosylation. These results suggest that approaches for predicting *O*-glycan structures in a sequence-specific manner may become a distinct possibility.

EXPERIMENTAL PROCEDURES

The site-specific PSM tandem repeat α-GalNAc and Core 1 glycosylation data obtained from three A blood-group minus pigs have been previously reported, Table 3 of ref *17*. The native and Core 1 data averaged over three individual PSM preparations were utilized in these calculations.

† Supported by the National Institutes of Health, National Cancer Institute, RO1-CA-78834.

* To whom correspondence should be addressed. Department of Pediatrics, Case Western Reserve University School of Medicine, BRB, Cleveland, OH 44106-4948. Telephone: 216-368-4556. Fax: 216-368-4223. E-mail: txg2@cwru.edu.

[1] Abbreviations: PSM, porcine salivary gland mucin; α-GalNAc, α-*N*-acetylgalactosamine; β-Gal, β-galactose; $k_{GalGalNAc}$, first-order rate constant for addition of Gal to GalNAc, see eq 1 in the Supporting Information; $W_{GalNAcn}$ and $W_{GalGalNAcn}$, GalNAc and Gal-GalNAc-disaccharide positional (*n*) weighting functions described in eqs 2 and 3 in the Supporting Information; *f*(GalNAc + GalGalNAc), modified exponential glycosylation density function described by eq 4 in the Supporting Information.

10.1021/bi036306a CCC: $27.50
Published on Web 03/16/2004

Kinetic modeling was performed using a modification of the approach developed for ppGalNAc transferases T1 and T2 (*19*) as described in detail in the Supporting Information. In the model, a global first-order rate constant for β-Gal addition to α-GalNAc, $k_{GalGalNAc}$, is multiplied by a factor, f(GalNAc + GalGalNAc) (ranging in value from 1 to 0), that is inversely proportional to the neighboring residue glycosylation state plus and minus three residues of the site of addition (see eqs 1−4 in the Supporting Information). As a result, the rate constant for glycosylation is decreased as a function of neighboring residue glycosylation. User adjustable positional-weighting coefficients $W_{GalNAcn}$ and $W_{GalGalNAcn}$ (where residue $n = -3$ to -1 and $+1$ to $+3$) are used to reflect the positional sensitivities of the Core 1 transferase to α-GalNAc and the Core 1 disaccharide (GalGalNAc) at each position, respectively. Values for $W_{GalNAcn}$ and $W_{GalGalNAcn}$ range from 0 to 1.0, representing no sensitivity to full sensitivity to glycosylation at the position n. The time course of glycosylation of α-GalNAc by β-Gal was obtained by numerical simulation of glycosylation kinetics (see eq 5 in the Supporting Information) using Lotus 123 spread sheet software release 9.7 (Lotus Development Corp., Cambridge, MA).

In this model, there are 13 adjustable variables (12 positional-weighting coefficients $W_{GalNAcn}$ and $W_{GalGalNAcn}$ and 1 rate constant $k_{GalGalNAc}$) for the fitting of 29 unique experimental data points. The implementation of this model involved the manual adjustment of the above variables until a satisfactory fit with the experimentally derived in vivo Core 1 glycosylation pattern was obtained. The fitting procedure began with systematically varying the positional-weighting functions (see below) and maximizing the fit (as monitored by the standard deviation SD and correlation coefficient r^2) for each weighting scheme by iterations on the $k_{GalGalNAc}$ value at a fixed arbitrary time point.[2] To further simplify the fitting procedure, the positional-weighting parameters were varied in 0.25 unit increments. Additional specific assumptions made in the implementation of this model are described in the results.

RESULTS

PSM Oligosaccharide Characterization. The O-linked glycans attached to the PSM 81 residue tandem repeat may range from mono- to pentasaccharide, representing the Tn through sialylated A blood-group antigenic determinates (see Figure 1; *20*−*22*). The site-specific in vivo glycosylation pattern of the PSM tandem repeat from a series of A blood-group minus pigs has recently been determined (*17*). In this paper and in an earlier study (*18*), it was observed that the basic α-GalNAc and Core 1 substitution patterns (β-Gal-(1−3) α-GalNAc-*O*-Ser/Thr) appeared to be nearly identical among individual pigs, while the subsequent formation of the H and A structures varied among individuals. This suggests similar expression levels of the core transferases and variable expression levels of the H and A blood-group synthesizing transferases among individuals. Analysis of the extent of Core 1 substitution revealed a weak inverse correlation (particularly with respect to Ser-linked glycans)

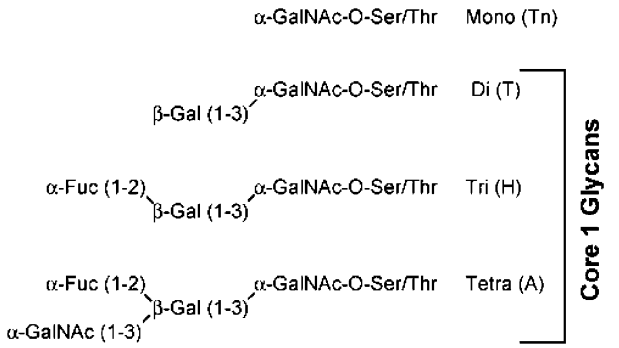

FIGURE 1: O-linked glycan structures found on the PSM (*20*−*22*). Core 1 glycans, defined by the β-(1−3) linked Gal, are indicated. The Core 1 glycosylation patterns characterized in this paper were derived from three A blood-group minus animals that lack the A blood-group tetrasaccharide (*17*). A sialic acid residue in the form of *N*-glycolylneuraminic acid (α-NeuNGl) may also be 2,6-linked to the peptide core α-GalNAc residue of each glycan.

with the density of Ser and Thr residues in the tandem repeat (see Figures 5B and 7A of ref *17*). These findings suggest that the Core 1 transferase may be inhibited by neighboring glycosylated residues. Because there is apparently one mammalian Core 1 transferase (UDP-galactose:glycoprotein-α-GalNAc β3-galactosyltransferase) (*23*−*25*),[3] it is reasonable to attempt to model the in vivo PSM Core 1 pattern using the kinetic modeling approach recently developed to model ppGalNAc transferases T1 and T2 (*19*).

Model Fitting the In Vivo PSM Core 1 Glycosylation Pattern. To model the in vivo Core 1 glycosylation pattern, a number of simplifying assumptions were made as follows: (1) that $k_{GalGalNAc}$ is identical for both Ser- and Thr-linked glycans (although a provision for differing rate constants is present); (2) that the in vivo Core 1 pattern represents a single arbitrary time point relatively advanced in the biosynthetic time course and calculated trajectory; (3) that the Core 1 transferase acts only after the full in vivo level of peptide-linked α-GalNAc is reached (i.e., there is no temporal competition among ppGalNAc and Core 1 transferases); (4) that there is no competing sialylation of the α-GalNAc residue; and (5) that further substitution of the Core 1 disaccharide will be invisible to the model (i.e., further substitution, occurring later in the biosynthetic pathway, does not compete temporally with the Core 1 formation). To simplify the initial fitting procedure, the positional-weighting values $W_{GalNAcn}$ and $W_{GalGalNAcn}$, representing the inhibitory effects of GalNAc and the Core 1 disaccharide, were assigned to identical values. This latter assumption reduced the number of unique fitting parameters to seven, excluding the arbitrarily chosen time point, which remained fixed.[2] The validity of many of these assumptions was further tested as discussed below.

After a systematic search process (see Figure S2 in the Supporting Information), a set of positional-weighting parameters was obtained that was found to optimally reproduce the in vivo Core 1 glycosylation pattern (Figure 2). Best results were obtained for $W_{GalNAcn}$ and $W_{GalGalNAcn}$ weights

[2] Note that the model fitting could have been equally performed using an arbitrarily fixed rate constant and performing iterations on the time-point value.

[3] Note that the second-described Core 1 transferase, Core 1 T2 (*25*), is not an active transferase because it has the identical amino acid sequence as the recently described Core 1 associated molecular chaperone, Cosmic, (*24*) that is required for the proper folding of the originally reported Core 1 transferase (*23*).

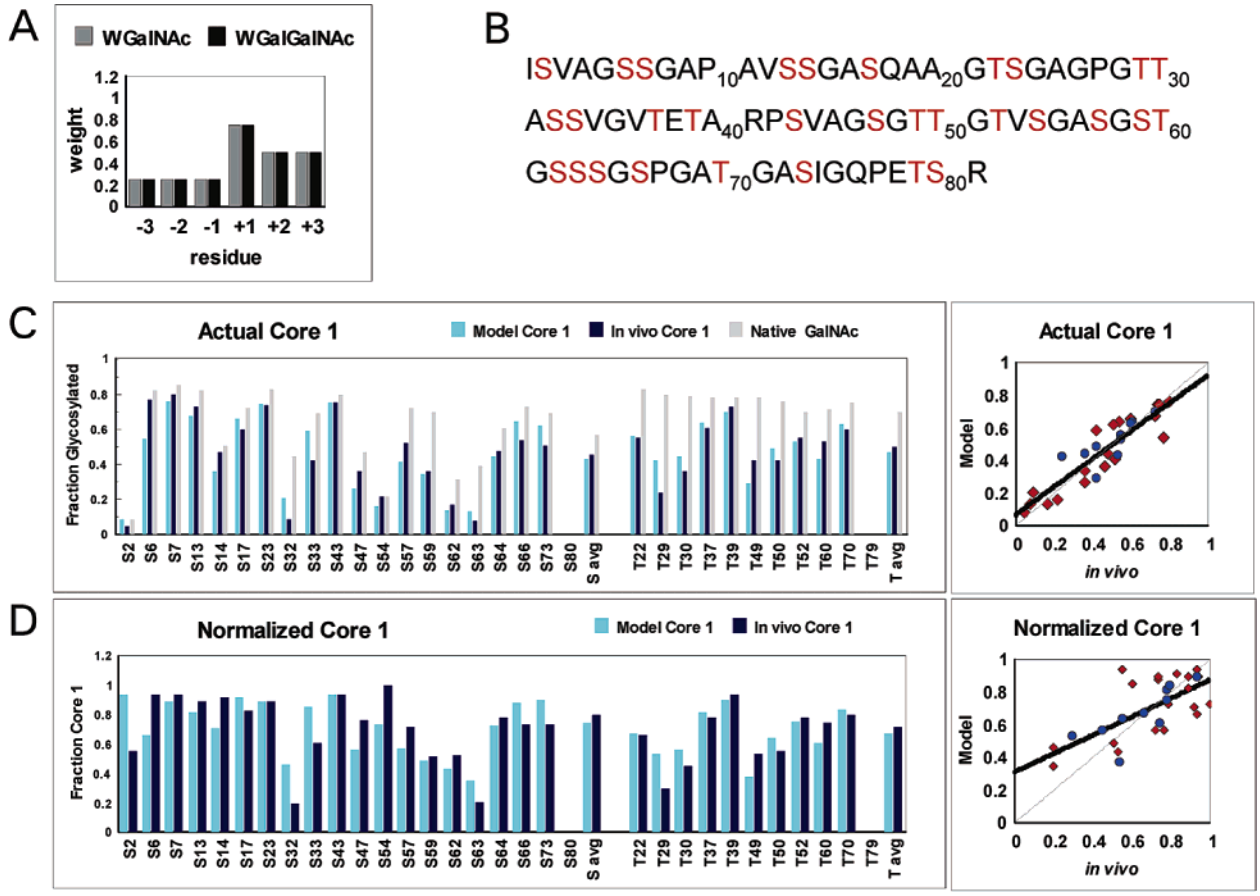

FIGURE 2: Results of the numerical simulation of the PSM tandem repeat in vivo Core 1 glycosylation pattern. (A) Optimized residue positional-weighting parameters, $W_{GalNAcn}$ and $W_{GalGalNAcn}$, employed in the calculation. (B) Amino acid sequence of the PSM 81 residue tryptic tandem repeat (*26*). Native mucin contains about 100 contiguous repeats of this sequence (*27*). (C) Left panel: Comparison of simulated (light blue bars) and experimental (dark blue bars) Core 1 glycosylation for Ser and Thr residues. The best fit gives a SD of 9.1 mol % for all residues (8.7 and 9.4 mol % for Ser and Thr separately). Also shown are the native peptide-linked α-GalNAc values for each residue (grey bars). Right panel: Plot of the calculated versus experimental Core 1 glycosylation (all points, $r^2 = 0.814$, slope = 0.854). Separate Ser data (red diamonds, $r^2 = 0.823$, slope = 0.872) and Thr data (blue circles, $r^2 = 0.604$, slope = 0.670) are given. (D) Left panel: Comparison of the normalized (relative to α-GalNAc) Core 1 glycosylation pattern (bars labeled the same as in C). Right panel: Plot of the normalized Core 1 data (all points, $r^2 = 0.469$, slope = 0.564). Separate Ser data ($r^2 = 0.407$, slope = 0.524) and Thr data ($r^2 = 0.635$, slope = 0.667) are labeled the same as in C. Note that data for Thr 79 and Ser 80 are omitted as their in vivo Core 1 data are uncertain. The exclusion of these data has no effect on modeling neighboring Ser 73 and is undetectable on Ser 2. The calculation was performed using a $k_{GalGalNAc}$ rate constant of 0.04 mole fraction/unit time and at the 70 unit time point (see the Supporting Information).

of 0.25, 0.25, 0.25, 0.75, 0.5, and 0.5 for the −3 to −1 and +1 to +3 positions relative to the site of glycosylation (Figure 2A). These weights give a model versus experiment standard deviation of 9.1 mol %, which is comparable to the estimated experimental error of the in vivo determinations. A comparison of the experimental and model Core 1 glycosylation for each Ser and Thr residue in the PSM tandem repeat is given in the left panel of Figure 2C. Each residue's native α-GalNAc glycosylation is also given in the figure. (Refer to Figure 2B for the complete sequence of the PSM tryptic tandem repeat (*26*, *27*).) A plot of the model versus in vivo Core 1 glycosylation gives a r^2 of 0.81 and slope of 0.85 (right panel of Figure 2C). Separate statistics for Ser- and Thr-linked glycans are given in the caption of Figure 2. Attempts to further improve the fitting by independently increasing the weights of the disaccharide, $W_{GalGalNAcn}$, failed to further improve the fit, typically resulting in poorer fits. In addition, poor fitting parameters were obtained when the monosaccharide $W_{GalNAcn}$ weights were zeroed, thereby fully placing the neighboring glycosylation effects onto the disaccharide (data not shown). As a validation of the model, no fitting parameters could be obtained that gave SD values below 15−20 mole percent after reversing the experimental Ser and Thr data in the sequence (data not shown). A failure to reproduce the out-of-sequence experimental data would be expected if Core 1 glycosylation was indeed modulated by neighboring glycosylation effects. Hence, the optimal fitting parameters obtained are not likely an artifact of the PSM sequence (see Table 2 in the Supporting Information of ref *19* for an analysis of the distribution of Ser and Thr residues in the sequence) nor of the fitting procedure.

To further evaluate the goodness of fit, corresponding plots of the Core 1 substitution patterns normalized to the initial α-GalNAc substitution were obtained (Figure 2D). With normalization, a less biased and more critical analysis of the simulation is obtained. However, with normalization, small differences within experimental error are emphasized for residues with low initial α-GalNAc contents, for example, Ser 2, 32, 54, and 63. Nevertheless, the plot of the normalized data (left panel of Figure 2D) demonstrates that the model quite satisfactorily represents the experimental glycosylation pattern. The plot of the normalized model versus experimental data give a r^2 of 0.47 and slope of 0.54 (right panel of Figure 2D).

An examination of the plots in parts C and D of Figure 2 reveals that the model is very capable of correctly reproducing the full range of observed Core 1 glycosylation values. For example, the experimentally observed low Core 1 glycosylation at Ser 32, 57, 59, 62, and 63 and Thr 22, 29, 30, 49, and 50 is predicted, while the high levels of glycosylation at the remaining residues are almost completely reproduced. Even for residues where the model and experimental values differ by greater than the estimated experimental error (~10−15 mol %), the model shows the correct high or low trend (i.e., Ser 6, Ser 33, and Thr 29).

DISCUSSION

O-glycosylation of Ser and Thr residues is initiated by the action of a family of Golgi resident ppGalNAc transferases (presently, ppGalNAc T1−T13), many of which possess unique ranges of peptide substrate preferences (*28*, *29*). *O*-glycan elongation continues in the Golgi by the action of a series of specific transferases that sequentially add sugars to the growing oligosaccharide side chain. The overall structural diversity observed for O-linked glycans has been attributed to many factors including the expression levels of transferases, the concentration of sugar nucleotide substrates, the sub-Golgi localization of transferases, and the competition of transferases for acceptor (for example, *30*−*34*). Except for the different peptide substrate preferences of the various ppGalNAc transferases [and their modulation by neighboring glycosylation (*19*, *35*)], none of these factors can readily account for the site-specific glycosylation patterns presently observed for longer O-linked glycans.

In this paper, the in vivo Core 1 glycosylation pattern of the PSM 81 residue tandem repeat has been reproduced using a kinetic model where the Core 1 transferase rate constant is decreased as a function of the extent of neighboring glycosylation. These results confirm previous suggestions (*17*, *18*) that Core 1 substitution may be modulated by neighboring glycosylation. Earlier Core 1 transferase studies, on short model peptide substrates, have also revealed suspected neighboring glycosylation effects as well other peptide-specific effects (i.e., charge and residue type) (*36*, *37*). However, the present paper suggests that, at least for heavily O-glycosylated mucin domains, neighboring glycosylation effects seem to dominate over the other factors, potentially modulating the formation of the Core 1 structures.

An analysis of the optimal positional-weighting parameters $W_{\mathrm{GalNAc}n}$ and $W_{\mathrm{GalGalNAc}n}$ (Figure 2A) reveals that the Core 1 transferase is weekly sensitive to the glycosylation of the three-residues N terminal of the site of glycosylation. In contrast, the transferase appears to be highly sensitive to the glycosylation of the adjacent residues C terminal of the glycosylation site. These effects may reflect the apparently fixed nature of the conformation of α-GalNAc residues attached to mucins and their effect on the conformation of the peptide core (*9*). It is noteworthy that the present model was found to produce the best fit under conditions where the transferase displayed identical sensitivities to neighboring α-GalNAc− and *β*-Gal(1−3) α-GalNAc−. These results suggest that the effects of neighboring α-GalNAc− (steric or conformational in nature) dominate and are not significantly increased upon elongation to the disaccharide. The model further suggests that the rates of Core 1 glycosylation of Ser- and Thr-linked α-GalNAc are identical. This contrasts with the earlier model peptide studies, which show Thr-linked α-GalNAc residues to be more rapidly glycosylated than Ser-linked glycans (*36*, *37*). However, native PSM does not display such a Thr/Ser Core 1 differential (see parts C and D of Figure 2); hence, the previous observations may be a result of the nature of the short ~8 residue glycopeptides utilized. Interestingly, however, the in vivo fucosylation of the PSM Core 1 structure shows a clear sensitivity to Ser- and Thr-linked glycans while showing no apparent sensitivity to neighboring group glycosylation (*17*). Studies in progress with purified Core 1 transferase on the PSM tandem repeat will further address both of the above uncertainties with the Core 1 transferase.

In the simulation, it was assumed that full peptide α-GalNAc addition was completed prior to Core 1 addition and that substitution by sialic acid did not compete or interfere with the formation of the Core 1 structure. The ability of the model to reasonably reproduce the in vivo Core 1 glycosylation suggests that many of these assumptions may possibly reflect the in vivo situation. Therefore, the apparent overlap of the Core 1 and ppGalNAc transferases in the cis Golgi may not necessarily preclude the possibility that substantial α-GalNAc addition can be achieved prior to *β*-Gal addition (*31*, *38*, *39*).[4] The assumption that sialylation does not compete with Core 1 glycosylation is consistent with sialyltransferases being typically localized to the trans Golgi (*32*, *40*). Likewise, the assumptions regarding the lack of temporal interference of the transferases that act on the Core 1 structure also seem reasonable.

To summarize, the site-specific in vivo Core 1 glycosylation pattern of the porcine submaxillary mucin tandem repeat has been reproduced by a simple kinetic modeling approach that takes into account an inhibitory effect of neighboring residue glycosylation. The model suggests that the peptide-linked α-GalNAc residue plays the dominant role in this inhibition. As a result, an important mechanism for the observed modulation of the Core 1 structures in vivo appears to have been elucidated. Although further detailed kinetic studies with purified transferase are desired to confirm these results in vitro, these findings suggest that the eventual ability to predict, by numerical kinetic modeling approaches, the initial core *O*-glycan patterns in mucin-like domains may be one step closer to fruition. With such models, it may become possible to elucidate the temporal activities and sub-Golgi localizations of the transferases involved in the initial steps of *O*-glycan biosynthesis.

SUPPORTING INFORMATION AVAILABLE

Description of the kinetic model and supporting Figures S1 and S2. This material is available free of charge via the Internet at http://pubs.acs.org.

[4] A ppGalNAc transferase (presumably T1) have been specifically localized to the cis Golgi apparatus in the mammalian salivary gland (*38*), while ppGalNAc T1, T2, and T3 have been differentially localized throughout the Golgi in HeLa cells (*39*). The Golgi localization of the Core 1 transferase has not been described; however, it must reside in the cis to medial Golgi with or before the major Core 2 *β*-*N*-acetylglucosaminyltransferase (C2GnT), whose substrate is the Core 1 structure (*31*).

REFERENCES

1. Van Klinken, B. J., Dekker, J., Buller, H. A., and Einerhand, A. W. (1995) Mucin gene structure and expression: Protection vs adheasion, *Am. J. Physiol. 269*, G613−G627.
2. Zheng, X., and Sadler, J. E. (2002) Mucin-like Domain of Enteropeptidase Directs Apical Targeting in Madin-Darby Canine Kidney Cells, *J. Biol. Chem. 277*, 6858−6863.
3. Rudd, P. M., Wormald, M. R., Stanfield, R. L., Huang, M., Mattsson, N., Speir, J. A., DiGennaro, J. A., Fetrow, J. S., Dwek, R. A., and Wilson, I. A. (1999) Roles for glycosylation of cell surface receptors involved in cellular immune recognition, *J. Mol. Biol. 293*, 351−366.
4. Fukuda, M., and Tsuboi, S. (1999) Mucin-type *O*-glycans and leukosialin, *Biochim. Biophys. Acta 1455*, 205−217.
5. Dennis, J. W., Granovsky, M., and Warren, C. E. (1999) Glycoprotein glycosylation and cancer progression, *Biochim. Biophys. Acta 1473*, 21−34.
6. Hanisch, F. G., and Muller, S. (2000) MUC1: the polymorphic appearance of a human mucin, *Glycobiology 10*, 439−449.
7. Tsuiji, H., Takasaki, S., Sakamoto, M., Irimura, T., and Hirohashi, S. (2003) Aberrant O-glycosylation inhibits stable expression of dysadherin, a carcinoma-associated antigen, and facilitates cell−cell adhesion, *Glycobiology 13*, 521.
8. Shogren, R., Gerken, T. A., and Jentoft, N. (1989) Role of glycosylation on the conformation and chain dimensions of O-linked glycoproteins: light-scattering studies of ovine submaxillary mucin, *Biochemistry 28*, 5525−5536.
9. Coltart, D. M., Royyuru, A. K., Williams, L. J., Glunz, P. W., Sames, D., Kuduk, S. D., Schwarz, J. B., Chen, X. T., Danishefsky, S. J., and Live, D. H. (2002) Principles of mucin architecture: structural studies on synthetic glycopeptides bearing clustered mono-, di-, tri-, and hexasaccharide glycodomains, *J. Am. Chem. Soc. 124*, 9833−9844.
10. Leppanen, A., White, S. P., Helin, J., McEver, R. P., and Cummings, R. D. (2000) Binding of Glycosulfopeptides to P-selectin Requires Stereospecific Contributions of Individual Tyrosine Sulfate and Sugar Residues, *J. Biol. Chem. 275*, 39569−39578.
11. Xu, Z., and Weiss, A. (2002) Negative regulation of CD45 by differential homodimerization of the alternatively spliced isoforms, *Nat. Immunol. 3*, 764−771.
12. Moody, A. M., Chui, D., Reche, P. A., Priatel, J. J., Marth, J. D., and Reinherz, E. L. (2001) Developmentally regulated glycosylation of the CD8αβ coreceptor stalk modulates ligand binding, *Cell 107*, 501−512.
13. Merry, A. H., Gilbert, R. J. C., Shore, D. A., Royle, L., Miroshnychenko, O., Vuong, M., Wormald, M. R., Harvey, D. J., Dwek, R. A., Classon, B. J., Rudd, P. M., and Davis, S. J. (2003) *O*-Glycan sialylation and the structure of the stalk-like region of the T cell co-receptor CD8, *J. Biol. Chem. 278*, 27119−27128.
14. Jacob, R., Preuss, U., Zimmer, K., Naim, H., and Naim, H. Y. (1999) O-linked glycans mediate apical sorting of human intestinal sucrase-isomaltase through association with lipid rafts, *Curr. Biol. 9*, 593−596.
15. Alfalah, M., Jacob, R., Preuss, U., Zimmer, K. P., Naim, H., and Naim, H. Y. (1999) O-linked glycans mediate apical sorting of human intestinal sucrase-isomaltase through association with lipid rafts, *Curr. Biol. 9*, 593−596.
16. Breuza, L., Garcia, M., Delgrossi, M. H., and Le Bivic, A. (2002) Role of the membrane-proximal O-glycosylation site in sorting of the human receptor for neurotrophins to the apical membrane of MDCK cells, *Exp. Cell Res. 273*, 178−186.
17. Gerken, T. A., Gilmore, M., and Zhang, J. (2002) Determination of the Site-specific Oligosaccharide Distribution of the *O*-Glycans Attached to the Porcine Submaxillary Mucin Tandem Repeat. Further evidence for the modulation of *O*-glycan side chain structures by peptide sequence, *J. Biol. Chem. 277*, 7736−7751.
18. Gerken, T. A., Owens, C. L., and Pasumarthy, M. (1998) Site-specific core 1 O-glycosylation pattern of the porcine submaxillary gland mucin tandem repeat. Evidence for the modulation of glycan length by peptide sequence, *J. Biol. Chem. 273*, 26580−26588.
19. Gerken, T. A., Zhang, J., Levine, J., and Elhammer, A. (2002) Mucin Core O-Glycosylation Is Modulated by Neighboring Residue Glycosylation Status. Kinetic modeling of the site-specific glycosylation of the apo-porcine submaxillary mucin tandem repeat by UDP-GalNAc: polypeptide *N*-acetylgalactosaminyltransferases T1 and T2, *J. Biol. Chem. 277*, 49850−49862.
20. Carlson, D. M. (1968) Structures and immunochemical properties of oligosaccharides isolated from pig submaxillary mucins, *J. Biol. Chem. 243*, 616−626.
21. Aminoff, D., Baig, M. M., and Gathmann, W. D. (1979) Glycoproteins and blood group activity. Oligosaccharides of A+ hog submaxillary glycoproteins, *J. Biol. Chem. 254*, 1788−1793.
22. van Halbeek, H., Dorland, L., Haverkamp, J., Veldink, G. A., Vliegenthart, J. F., Fournet, B., Ricart, G., Montreuil, J., Gathmann, W. D., and Aminoff, D. (1981) Structure determination of oligosaccharides isolated from A+, H+ and A−H− hog-submaxillary-gland mucin glycoproteins, by 360-MHz 1H NMR spectroscopy, permethylation analysis and mass spectrometry, *Eur. J. Biochem. 118*, 487−495.
23. Ju, T., Brewer, K., D′Souza, A., Cummings, R. D., and Canfield, W. M. (2001) Cloning and Expression of Human Core 1 β 1,3-Galactosyltransferase, *J. Biol. Chem. 277*, 178−186.
24. Ju, T., and Cummings, R. D. (2002) A unique molecular chaperone Cosmc required for activity of the mammalian core 1 beta 3-galactosyltransferase, *Proc. Natl. Acad. Sci. U.S.A. 99*, 16613−16618.
25. Kudo, T., Iwai, T., Kubota, T., Iwasaki, H., Hiruma, T., Inaba, N., Zhang, Y., Gotoh, M., Togayachi, A., and Narimatsu, H. (2002) Molecular cloning and characterization of a novel UDP-Gal: GalNAca-peptide β1,3-galactosyltransferase (C1Gal-T2), an enzyme synthesizing a core 1 structure of *O*-glycan, *J. Biol. Chem. 277*, 47724−47731.
26. Timpte, C. S., Eckhardt, A. E., Abernethy, J. L., and Hill, R. L. (1988) Porcine submaxillary gland apomucin contains tandemly repeated, identical sequences of 81 residues, *J. Biol. Chem. 263*, 1081−1088.
27. Eckhardt, A. E., Timpte, C. S., DeLuca, A. W., and Hill, R. L. (1997) The Complete cDNA Sequence and Structural Polymorphism of the Polypeptide Chain of Porcine Submaxillary Mucin, *J. Biol. Chem. 272*, 33204−33210.
28. Schwientek, T. J., Bennett, E. P., Flores, C., Thacker, J., Hollman, M., Reis, C. A., Behrens, J., Mandel, U., Keck, B., Schafer, M. A., Hazelmann, K., Zubarev, R., Roepstorff, P., Hollingsworth, M. A., and Clausen, H. (2002) Functional conservation of subfamilies of putative UDP-*N*-acetylgalactosamine: Polypeptide *N*-acetylgalactosaminyltransferases in drosophila, *C. elegans* and mammals: One subfamily comprised of l(2)35Aa is essential in *drosophila*, *J. Biol. Chem. 277*, 22623−22638.
29. Ten Hagen, K. G., Fritz, T. A., and Tabak, L. A. (2003) "All in the Family"—The UDP-GalNAc:polypeptide *N*-acetylgalactosaminyltransferases, *Glycobiology 13*, 1R−16R.
30. Van den Steen, P. E., Rudd, P. M., Dwek, R. A., and Opdenakker, G. (1998) Concepts and principles of O-linked glycosylation, *Crit. Rev. Biochem. Mol. Biol. 33*, 151−208.
31. Dalziel, M., Whitehouse, C., McFarlane, I., Brockhausen, I., Gschmeissner, S., Schwientek, T., Clausen, H., Burchell, J. M., and Taylor-Papadimitriou, J. (2001) The Relative Activities of the C2GnT1 and ST3Gal-I Glycosyltransferases Determine *O*-Glycan Structure and Expression of a Tumor-associated Epitope on MUC1, *J. Biol. Chem. 276*, 11007−11015.
32. Whitehouse, C., Burchell, J., Gschmeissner, S., Brockhausen, I., Lloyd, K. O., and Taylor-Papadimitriou, J. (1997) A Transfected Sialyltransferase That Is Elevated in Breast Cancer and Localizes to the medial/trans-Golgi Apparatus Inhibits the Development of core-2-based *O*-Glycans, *J. Cell Biol. 137*, 1229.
33. Skrincosky, D., Kain, R., El Battari, A., Exner, M., Kerjaschki, D., and Fukuda, M. (1997) Altered Golgi Localization of Core 2 β-1,6-*N*-Acetylglucosaminyltransferase Leads to Decreased Synthesis of Branched *O*-Glycans, *J. Biol. Chem. 272*, 22695−22702.
34. Hanisch, F. G. (2001) O-glycosylation of the mucin type, *Biol. Chem. 382*, 143−149.
35. Hanisch, F. G., Reis, C. A., Clausen, H., and Paulsen, H. (2001) Evidence for glycosylation-dependent activities of polypeptide *N*-acetylgalactosaminyltransferases rGalNAc-T2 and -T4 on mucin glycopeptides, *Glycobiology 11*, 731−740.
36. Brockhausen, I., Moller, G., Merz, G., Adermann, K., and Paulsen, H. (1990) Control of mucin synthesis: the peptide portion of synthetic O-glycopeptide substrates influences the activity of *O*-glycan core 1 UDPgalactose: *N*-acetyl-α-galactosaminyl-R β 3-galactosyltransferase, *Biochemistry 29*, 10206−10212.
37. Granovsky, M., Bielfeldt, T., Peters, S., Paulsen, H., Meldal, M., Brockhausen, J., and Brockhausen, I. (1994) UDP-galactose: glycoprotein-*N*-acetyl-D-galactosamine 3-β-D-galactosyltransferase activity synthesizing *O*-glycan core 1 is controlled by the amino acid sequence and glycosylation of glycopeptide substrates, *Eur. J. Biochem. 221*, 1039−1046.

38. Roth, J., Wang, Y., Eckhardt, A. E., and Hill, R. L. (1994) Subcellular localization of the UDP-*N*-acetyl-D-galactosamine: polypeptide *N*-acetylgalactosaminyltransferase-mediated O-glycosylation reaction in the submaxillary gland, *Proc. Natl. Acad. Sci. U.S.A. 91*, 8935−8939.
39. Rottger, S., White, J., Wandall, H. H., Olivo, J. C., Stark, A., Bennett, E. P., Whitehouse, C., Berger, E. G., Clausen, H., and Nilsson, T. (1998) Localization of three human polypeptide GalNAc-transferases in HeLa cells suggests initiation of O-linked glycosylation throughout the Golgi apparatus, *J. Cell Sci. 111*, 45−60.
40. Breton, C., Mucha, J., and Jeanneau, C. (2001) Structural and functional features of glycosyltransferases, *Biochimie 83*, 713−718.

BI036306A